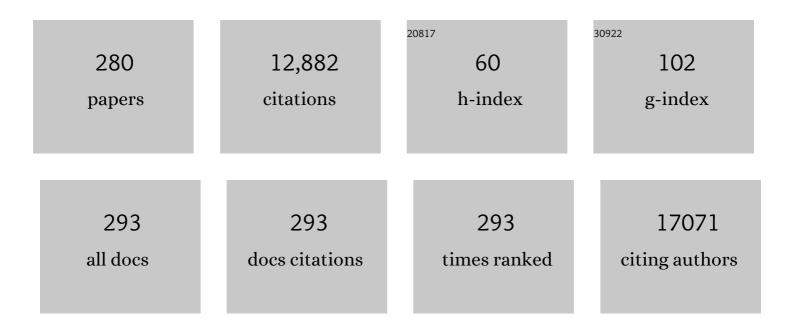
## Hyungjun Kim

List of Publications by Year in descending order

Source: https://exaly.com/author-pdf/187975/publications.pdf Version: 2024-02-01



Нунисины Кім

#	Article	IF	CITATIONS
1	On the importance of the electric double layer structure in aqueous electrocatalysis. Nature Communications, 2022, 13, 174.	12.8	92
2	BitBlade: Energy-Efficient Variable Bit-Precision Hardware Accelerator for Quantized Neural Networks. IEEE Journal of Solid-State Circuits, 2022, 57, 1924-1935.	5.4	11
3	A bimetallic PdCu–Fe <sub>3</sub> O <sub>4</sub> catalyst with an optimal d-band centre for selective <i>N</i> -methylation of aromatic amines with methanol. Catalysis Science and Technology, 2022, 12, 3524-3533.	4.1	6
4	Enhanced Light Emission through Symmetry Engineering of Halide Perovskites. Journal of the American Chemical Society, 2022, 144, 297-305.	13.7	5
5	Development of RuS2 for near-infrared photodetector by atomic layer deposition and post-sulfurization. Rare Metals, 2022, 41, 3086-3099.	7.1	4
6	MoS2 doping by atomic layer deposition of high-k dielectrics using alcohol as process oxidants. Applied Surface Science, 2021, 541, 148504.	6.1	6
7	PE-ALD of Ge <sub>1â^'x</sub> S <sub>x</sub> amorphous chalcogenide alloys for OTS applications. Journal of Materials Chemistry C, 2021, 9, 6006-6013.	5.5	12
8	Unipolar stroke, electroosmotic pump carbon nanotube yarn muscles. Science, 2021, 371, 494-498.	12.6	110
9	Dynamic Transformation of a Ag <sup>+</sup> -Coordinated Supramolecular Nanostructure from a 1D Needle to a 1D Helical Tube via a 2D Ribbon Accompanying the Conversion of Complex Structures. Journal of the American Chemical Society, 2021, 143, 3113-3123.	13.7	24
10	Selective electrochemical reduction of nitric oxide to hydroxylamine by atomically dispersed iron catalyst. Nature Communications, 2021, 12, 1856.	12.8	106
11	2D MoS <sub>2</sub> Charge Injection Memory Transistors Utilizing Heteroâ€Stack SiO <sub>2</sub> /HfO <sub>2</sub> Dielectrics and Oxide Interface Traps. Advanced Electronic Materials, 2021, 7, 2100074.	5.1	8
12	Atomic‣ayerâ€Depositionâ€Based 2D Transition Metal Chalcogenides: Synthesis, Modulation, and Applications. Advanced Materials, 2021, 33, e2005907.	21.0	42
13	Lattice Engineering to Simultaneously Control the Defect/Stacking Structures of Layered Double Hydroxide Nanosheets to Optimize Their Energy Functionalities. ACS Nano, 2021, 15, 8306-8318.	14.6	49
14	Hydrogen Barriers Based on Chemical Trapping Using Chemically Modulated Al <sub>2</sub> O <sub>3</sub> Grown by Atomic Layer Deposition for InGaZnO Thin-Film Transistors. ACS Applied Materials & Interfaces, 2021, 13, 20349-20360.	8.0	15
15	Femtosecond Quantum Dynamics of Excited-State Evolution of Halide Perovskites: Quantum Chaos of Molecular Cations. Journal of Physical Chemistry C, 2021, 125, 10676-10684.	3.1	1
16	Microbially Guided Discovery and Biosynthesis of Biologically Active Natural Products. ACS Synthetic Biology, 2021, 10, 1505-1519.	3.8	11
17	Interface Defect Engineering of a Largeâ€Scale CVDâ€Grown MoS <sub>2</sub> Monolayer via Residual Sodium at the SiO <sub>2</sub> /Si Substrate. Advanced Materials Interfaces, 2021, 8, 2100428.	3.7	14
18	Physicochemical Understanding of the Impact of Pore Environment and Species of Adsorbates on Adsorption Behaviour. Angewandte Chemie, 2021, 133, 20667-20673.	2.0	1

#	Article	IF	CITATIONS
19	Simultaneous Enhanced Efficiency and Stability of Perovskite Solar Cells Using Adhesive Fluorinated Polymer Interfacial Material. ACS Applied Materials & Interfaces, 2021, 13, 35595-35605.	8.0	20
20	Physicochemical Understanding of the Impact of Pore Environment and Species of Adsorbates on Adsorption Behaviour. Angewandte Chemie - International Edition, 2021, 60, 20504-20510.	13.8	8
21	Interface Defect Engineering of MoS <sub>2</sub> Monolayer: Interface Defect Engineering of a Large cale CVDâ€Grown MoS <sub>2</sub> Monolayer via Residual Sodium at the SiO <sub>2</sub> /Si Substrate (Adv. Mater. Interfaces 14/2021). Advanced Materials Interfaces, 2021, 8, 2170080.	3.7	1
22	Assessment and prediction of band edge locations of nitrides using a self-consistent hybrid functional. Journal of Chemical Physics, 2021, 155, 024120.	3.0	1
23	Synthesis and Application of AgBiS <sub>2</sub> and Ag <sub>2</sub> S Nanoinks for the Production of IR Photodetectors. ACS Omega, 2021, 6, 20710-20718.	3.5	19
24	Reaction Mechanisms of Non-hydrolytic Atomic Layer Deposition of Al <sub>2</sub> O <sub>3</sub> with a Series of Alcohol Oxidants. Journal of Physical Chemistry C, 2021, 125, 18151-18160.	3.1	6
25	Growth mechanism and electrical properties of tungsten films deposited by plasma-enhanced atomic layer deposition with chloride and metal organic precursors. Applied Surface Science, 2021, 568, 150939.	6.1	5
26	Optical Reflection from Unforbidden Diffraction of Block Copolymer Templated Gyroid Films. ACS Macro Letters, 2021, 10, 1609-1615.	4.8	6
27	Group IV Transition Metal (M = Zr, Hf) Precursors for High-κ Metal Oxide Thin Films. Inorganic Chemistry, 2021, 60, 17722-17732.	4.0	4
28	Photocurrent Enhancement of PtSe2 Photodetectors by Using Au Nanorods. Photonics, 2021, 8, 505.	2.0	7
29	<i>In Situ</i> Mapping and Local Negative Uptake Behavior of Adsorbates in Individual Pores of Metal–Organic Frameworks. Journal of the American Chemical Society, 2021, 143, 20747-20757.	13.7	5
30	uMBD: A Materials-Ready Dispersion Correction That Uniformly Treats Metallic, Ionic, and van der Waals Bonding. Journal of the American Chemical Society, 2020, 142, 2346-2354.	13.7	29
31	Surface Energy Change of Atomic-Scale Metal Oxide Thin Films by Phase Transformation. ACS Nano, 2020, 14, 676-687.	14.6	10
32	Comparative study on atomic layer deposition of HfO <sub>2</sub> <i>via</i> substitution of ligand structure with cyclopentadiene. Journal of Materials Chemistry C, 2020, 8, 1344-1352.	5.5	24
33	Rate performance enhancement of lithium-ion battery using precise thickness-controllable-carbon-coated titanium dioxide nanowire array electrode via atomic layer deposition. Electrochimica Acta, 2020, 334, 135596.	5.2	9
34	Atomic layer deposition for nonconventional nanomaterials and their applications. Journal of Materials Research, 2020, 35, 656-680.	2.6	9
35	A General Strategy to Atomically Dispersed Precious Metal Catalysts for Unravelling Their Catalytic Trends for Oxygen Reduction Reaction. ACS Nano, 2020, 14, 1990-2001.	14.6	116
36	Activity–Stability Relationship in Au@Pt Nanoparticles for Electrocatalysis. ACS Energy Letters, 2020, 5, 2827-2834.	17.4	49

#	Article	IF	CITATIONS
37	Selfâ€Powered Gas Sensors: 2D Transition Metal Dichalcogenide Heterostructures for p―and nâ€īype Photovoltaic Selfâ€Powered Gas Sensor (Adv. Funct. Mater. 43/2020). Advanced Functional Materials, 2020, 30, 2070284.	14.9	1
38	Thermal Transformation of Molecular Ni <sup>2+</sup> –N <sub>4</sub> Sites for Enhanced CO <sub>2</sub> Electroreduction Activity. ACS Catalysis, 2020, 10, 10920-10931.	11.2	81
39	Intermetallic PtCu Nanoframes as Efficient Oxygen Reduction Electrocatalysts. Nano Letters, 2020, 20, 7413-7421.	9.1	109
40	Fe <sub><i>x</i></sub> Ni <sub>2–<i>x</i></sub> P Alloy Nanocatalysts with Electron-Deficient Phosphorus Enhancing the Hydrogen Evolution Reaction in Acidic Media. ACS Catalysis, 2020, 10, 11665-11673.	11.2	41
41	2D Transition Metal Dichalcogenide Heterostructures for p―and nâ€Type Photovoltaic Selfâ€Powered Gas Sensor. Advanced Functional Materials, 2020, 30, 2003360.	14.9	102
42	Electric Field Mediated Selectivity Switching of Electrochemical CO <sub>2</sub> Reduction from Formate to CO on Carbon Supported Sn. ACS Energy Letters, 2020, 5, 2987-2994.	17.4	41
43	Water Slippage on Graphitic and Metallic Surfaces: Impact of the Surface Packing Structure and Electron Density Tail. Journal of Physical Chemistry C, 2020, 124, 11392-11400.	3.1	6
44	Atomic layer deposition of a uniform thin film on two-dimensional transition metal dichalcogenides. Journal of Vacuum Science and Technology A: Vacuum, Surfaces and Films, 2020, 38, .	2.1	25
45	Monolayered g-C3N4 nanosheet as an emerging cationic building block for bifunctional 2D superlattice hybrid catalysts with controlled defect structures. Applied Catalysis B: Environmental, 2020, 277, 119191.	20.2	56
46	Dynamic metal-polymer interaction for the design of chemoselective and long-lived hydrogenation catalysts. Science Advances, 2020, 6, eabb7369.	10.3	53
47	Synthesis of a Hybrid Nanostructure of ZnO-Decorated MoS <sub>2</sub> by Atomic Layer Deposition. ACS Nano, 2020, 14, 1757-1769.	14.6	29
48	Improved interface quality of atomic-layer-deposited ZrO2 metal-insulator-metal capacitors with Ru bottom electrodes. Thin Solid Films, 2020, 701, 137950.	1.8	14
49	Thermodynamics of Multicomponent Perovskites: A Guide to Highly Efficient and Stable Solar Cell Materials. Chemistry of Materials, 2020, 32, 4265-4272.	6.7	26
50	The Precursor Adsorption Mechanism, Growth Characteristics and Electrical Properties of Plasma-Enhanced Atomic Layer Deposited Tungsten Films by Using Tungsten Chloride Precursors. , 2020, , .		0
51	Comparative Study of the Growth Characteristics and Electrical Properties of Atomic-layer-deposited W Films Obtained from Newly Synthesized Metalorganic and Halide Precursor. , 2020, , .		0
52	Synthesis of two-dimensional MoS2/graphene heterostructure by atomic layer deposition using MoF6 precursor. Applied Surface Science, 2019, 494, 591-599.	6.1	25
53	Porous Metal–Organic Framework CUK-1 for Adsorption Heat Allocation toward Green Applications of Natural Refrigerant Water. ACS Applied Materials & Interfaces, 2019, 11, 25778-25789.	8.0	45
54	Improved Sensitivity in Schottky Contacted Two-Dimensional MoS <sub>2</sub> Gas Sensor. ACS Applied Materials & Interfaces, 2019, 11, 38902-38909.	8.0	117

#	Article	IF	CITATIONS
55	Selectivity Modulated by Surface Ligands on Cu <sub>2</sub> O/TiO <sub>2</sub> Catalysts for Gas-Phase Photocatalytic Reduction of Carbon Dioxide. Journal of Physical Chemistry C, 2019, 123, 29184-29191.	3.1	27
56	Activity Origin and Multifunctionality of Pt-Based Intermetallic Nanostructures for Efficient Electrocatalysis. ACS Catalysis, 2019, 9, 11242-11254.	11.2	96
57	Thickness-dependent electrochemical response of plasma enhanced atomic layer deposited WS2 anodes in Na-ion battery. Electrochimica Acta, 2019, 322, 134766.	5.2	18
58	Textile-based high-performance hydrogen evolution of low-temperature atomic layer deposition of cobalt sulfide. Nanoscale, 2019, 11, 844-850.	5.6	17
59	Hydrogen barrier performance of sputtered La2O3 films for InGaZnO thin-film transistor. Journal of Materials Science, 2019, 54, 11145-11156.	3.7	18
60	Moisture barrier properties of low-temperature atomic layer deposited Al2O3 using various oxidants. Ceramics International, 2019, 45, 19105-19112.	4.8	11
61	Ligand-Controlled Direct Hydroformylation of Trisubstituted Olefins. Organic Letters, 2019, 21, 5789-5792.	4.6	17
62	Experimental and Density Functional Theory Corroborated Optimization of Durable Metal Embedded Carbon Nanofiber for Oxygen Electrocatalysis. Journal of Physical Chemistry Letters, 2019, 10, 3109-3114.	4.6	16
63	Out-of-plane piezoresponse of monolayer MoS2 on plastic substrates enabled by highly uniform and layer-controllable CVD. Applied Surface Science, 2019, 487, 1356-1361.	6.1	36
64	Phase-controlled synthesis of SnOx thin films by atomic layer deposition and post-treatment. Applied Surface Science, 2019, 480, 472-477.	6.1	25
65	Low-temperature, high-growth-rate ALD of SiO2 using aminodisilane precursor. Applied Surface Science, 2019, 485, 381-390.	6.1	27
66	Light Emission Enhancement by Tuning the Structural Phase of APbBr <sub>3</sub> (A =) Tj ETQq0 0 0 rgBT /Ove 2135-2142.	erlock 10 1 4.6	f 50 307 Td 12
67	Enthalpy–Entropy Interplay in π-Stacking Interaction of Benzene Dimer in Water. Journal of Chemical Theory and Computation, 2019, 15, 1538-1545.	5.3	16
68	Bi-layer high- <i>k</i> dielectrics of Al <sub>2</sub> O <sub>3</sub> /ZrO <sub>2</sub> to reduce damage to MoS <sub>2</sub> channel layers during atomic layer deposition. 2D Materials, 2019, 6, 015019.	4.4	12
69	Probing Surface Chemistry at an Atomic Level: Decomposition of 1-Propanethiol on GaP(001) (2 × 4) Investigated by STM, XPS, and DFT. Journal of Physical Chemistry C, 2019, 123, 2964-2972.	3.1	0
70	Atomic Layer Deposition of Al2O3 with Alcohol Oxidants for Impeding Substrate Oxidation. ECS Meeting Abstracts, 2019, , .	0.0	0
71	Hydrogen Barrier Properties of Atomic Layer Deposited Al <sub>2</sub> O <sub>3</sub> with Different Oxidants for Ingazno Thin Film Transistor. ECS Meeting Abstracts, 2019, MA2019-02, 1129-1129.	0.0	2
72	Interlayer-assisted atomic layer deposition of MgO as a magnetic tunneling junction insulators. Journal of Alloys and Compounds, 2018, 747, 505-510.	5.5	7

#	Article	IF	CITATIONS
73	Improved Synapse Device With MLC and Conductance Linearity Using Quantized Conduction for Neuromorphic Systems. IEEE Electron Device Letters, 2018, 39, 312-315.	3.9	60
74	High-Performance Ink-Synthesized Cu-Gate Thin-Film Transistor with Diffusion Barrier Formation. Metals and Materials International, 2018, 24, 652-656.	3.4	1
75	Cluster Expansion Method for Simulating Realistic Size of Nanoparticle Catalysts with an Application in CO <sub>2</sub> Electroreduction. Journal of Physical Chemistry C, 2018, 122, 9245-9254.	3.1	17
76	Polymeric Carbon Nitride with Localized Aluminum Coordination Sites as a Durable and Efficient Photocatalyst for Visible Light Utilization. ACS Catalysis, 2018, 8, 4241-4256.	11.2	118
77	Mixed Valence Perovskite Cs <sub>2</sub> Au <sub>2</sub> I <sub>6</sub> : A Potential Material for Thinâ€Film Pbâ€Free Photovoltaic Cells with Ultrahigh Efficiency. Advanced Materials, 2018, 30, e1707001.	21.0	79
78	Insight into the Microenvironments of the Metal–Ionic Liquid Interface during Electrochemical CO <sub>2</sub> Reduction. ACS Catalysis, 2018, 8, 2420-2427.	11.2	77
79	Exfoliated 2D Lepidocrocite Titanium Oxide Nanosheets for High Sulfur Content Cathodes with Highly Stable Li–S Battery Performance. ACS Energy Letters, 2018, 3, 412-419.	17.4	90
80	Enhanced Light Stability of InGaZnO Thin-Film Transistors by Atomic-Layer-Deposited Y <sub>2</sub> O <sub>3</sub> with Ozone. ACS Applied Materials & Interfaces, 2018, 10, 2143-2150.	8.0	41
81	Water-Erasable Memory Device for Security Applications Prepared by the Atomic Layer Deposition of GeO <sub>2</sub> . Chemistry of Materials, 2018, 30, 830-840.	6.7	15
82	Hydrogen plasma-enhanced atomic layer deposition of hydrogenated amorphous carbon thin films. Surface and Coatings Technology, 2018, 344, 12-20.	4.8	9
83	Ga–Doped Pt–Ni Octahedral Nanoparticles as a Highly Active and Durable Electrocatalyst for Oxygen Reduction Reaction. Nano Letters, 2018, 18, 2450-2458.	9.1	125
84	Multiscale Simulation Method for Quantitative Prediction of Surface Wettability at the Atomistic Level. Journal of Physical Chemistry Letters, 2018, 9, 1750-1758.	4.6	23
85	Bifunctional 2D Superlattice Electrocatalysts of Layered Double Hydroxide–Transition Metal Dichalcogenide Active for Overall Water Splitting. ACS Energy Letters, 2018, 3, 952-960.	17.4	140
86	Cobalt titanium nitride amorphous metal alloys by atomic layer deposition. Journal of Alloys and Compounds, 2018, 737, 684-692.	5.5	5
87	Input-Splitting of Large Neural Networks for Power-Efficient Accelerator with Resistive Crossbar Memory Array. , 2018, , .		17
88	Roles of SnX <sub>2</sub> (X = F, Cl, Br) Additives in Tin-Based Halide Perovskites toward Highly Efficient and Stable Lead-Free Perovskite Solar Cells. Journal of Physical Chemistry Letters, 2018, 9, 6024-6031.	4.6	121
89	Superior role of MXene nanosheet as hybridization matrix over graphene in enhancing interfacial electronic coupling and functionalities of metal oxide. Nano Energy, 2018, 53, 841-848.	16.0	36
90	Effects of Ar Addition to O <sub>2</sub> Plasma on Plasma-Enhanced Atomic Layer Deposition of Oxide Thin Films. ACS Applied Materials & Interfaces, 2018, 10, 40286-40293.	8.0	14

#	Article	IF	CITATIONS
91	High-Performance Gas Sensor Using a Large-Area WS <sub>2<i>x</i></sub> Se <sub>2–2<i>x</i></sub> Alloy for Low-Power Operation Wearable Applications. ACS Applied Materials & Interfaces, 2018, 10, 34163-34171.	8.0	93
92	Simultaneous improvement of the dielectric constant and leakage currents of ZrO <sub>2</sub> dielectrics by incorporating a highly valent Ta <sup>5+</sup> element. Journal of Materials Chemistry C, 2018, 6, 9794-9801.	5.5	13
93	Recovery Improvement for Large-Area Tungsten Diselenide Gas Sensors. ACS Applied Materials & Interfaces, 2018, 10, 23910-23917.	8.0	115
94	Comparative study of the growth characteristics and electrical properties of atomic-layer-deposited HfO <sub>2</sub> films obtained from metal halide and amide precursors. Journal of Materials Chemistry C, 2018, 6, 7367-7376.	5.5	40
95	Molecular oxidation of surface –CH3 during atomic layer deposition of Al2O3 with H2O, H2O2, and O3: A theoretical study. Applied Surface Science, 2018, 457, 376-380.	6.1	29
96	Structural and electrical properties of Ge-doped ZrO2 thin films grown by atomic layer deposition for high-k dielectrics. Journal of Materials Science, 2018, 53, 15237-15245.	3.7	18
97	Low-temperature direct synthesis of high quality WS2 thin films by plasma-enhanced atomic layer deposition for energy related applications. Applied Surface Science, 2018, 459, 596-605.	6.1	42
98	Low-temperature synthesis of 2D MoS <sub>2</sub> on a plastic substrate for a flexible gas sensor. Nanoscale, 2018, 10, 9338-9345.	5.6	142
99	Molecular Identification of Cr(VI) Removal Mechanism on Vivianite Surface. Environmental Science & Technology, 2018, 52, 10647-10656.	10.0	53
100	Amorphous TiO2/p-Si Heterojunction Photodiode Prepared by Low-Temperature Atomic Layer Deposition. Nanoscience and Nanotechnology Letters, 2018, 10, 800-804.	0.4	2
101	Surface Wettability of Nitrogen-Doped TiO2 Films Prepared by Atomic Layer Deposition Using NH4OH as the Doping Source. Nanoscience and Nanotechnology Letters, 2018, 10, 779-783.	0.4	1
102	A composite layer of atomic-layer-deposited Al2O3 and graphene for flexible moisture barrier. Carbon, 2017, 116, 553-561.	10.3	45
103	Growth behavior of Bi <sub>2</sub> Te <sub>3</sub> and Sb <sub>2</sub> Te <sub>3</sub> thin films on graphene substrate grown by plasma-enhanced chemical vapor deposition. Physica Status Solidi - Rapid Research Letters, 2017, 11, 1600369.	2.4	11
104	Polymorphic Phase Control Mechanism of Organic–Inorganic Hybrid Perovskite Engineered by Dual-Site Alloying. Journal of Physical Chemistry C, 2017, 121, 9508-9515.	3.1	16
105	Improvement of thermoelectric properties of Bi <sub>2</sub> Te <sub>3</sub> and Sb <sub>2</sub> Te <sub>3</sub> films grown on graphene substrate. Physica Status Solidi - Rapid Research Letters, 2017, 11, 1700029.	2.4	14
106	Comparative study on growth characteristics and electrical properties of ZrO2 films grown using pulsed plasma-enhanced chemical vapor deposition and plasma-enhanced atomic layer deposition for oxide thin film transistors. Journal of Vacuum Science and Technology A: Vacuum, Surfaces and Films, 2017, 35, 031510.	2.1	4
107	Facile CO <sub>2</sub> Electro-Reduction to Formate via Oxygen Bidentate Intermediate Stabilized by High-Index Planes of Bi Dendrite Catalyst. ACS Catalysis, 2017, 7, 5071-5077.	11.2	263
108	Atomic layer deposition of Y-stabilized ZrO2 for advanced DRAM capacitors. Journal of Alloys and Compounds, 2017, 722, 307-312.	5.5	40

#	Article	IF	CITATIONS
109	Fabrication of single-phase SnS film by H2 annealing of amorphous SnSx prepared by atomic layer deposition. Journal of Vacuum Science and Technology A: Vacuum, Surfaces and Films, 2017, 35, .	2.1	17
110	Growth mechanism of Co thin films formed by plasma-enhanced atomic layer deposition using NH3 as plasma reactant. Current Applied Physics, 2017, 17, 333-338.	2.4	14
111	Distorted Carbon Nitride Structure with Substituted Benzene Moieties for Enhanced Visible Light Photocatalytic Activities. ACS Applied Materials & Interfaces, 2017, 9, 40360-40368.	8.0	80
112	Atomistic Simulation Protocol for Improved Design of Si–O–C Hybrid Nanostructures as Li-Ion Battery Anodes: ReaxFF Reactive Force Field. Journal of Physical Chemistry C, 2017, 121, 23268-23275.	3.1	14
113	Catalytic chemical vapor deposition of large-area uniform two-dimensional molybdenum disulfide using sodium chloride. Nanotechnology, 2017, 28, 465103.	2.6	42
114	New Features and Uncovered Benefits of Polycrystalline Magnetite as Reusable Catalyst in Reductive Chemical Conversion. Journal of Physical Chemistry C, 2017, 121, 25195-25205.	3.1	15
115	Micropatternable Double-Faced ZnO Nanoflowers for Flexible Gas Sensor. ACS Applied Materials & Interfaces, 2017, 9, 32876-32886.	8.0	147
116	Surface-Localized Sealing of Porous Ultralow- <i>k</i> Dielectric Films with Ultrathin (<2 nm) Polymer Coating. ACS Nano, 2017, 11, 7841-7847.	14.6	19
117	The Impact of an Ultrathin Y <sub>2</sub> O <sub>3</sub> Layer on GeO <sub>2</sub> Passivation in Ge MOS Gate Stacks. IEEE Transactions on Electron Devices, 2017, 64, 3303-3307.	3.0	19
118	Input Voltage Mapping Optimized for Resistive Memory-Based Deep Neural Network Hardware. IEEE Electron Device Letters, 2017, 38, 1228-1231.	3.9	37
119	Atomic-scale characterization of plasma-induced damage in plasma-enhanced atomic layer deposition. Applied Surface Science, 2017, 425, 781-787.	6.1	6
120	Transfer and Dynamic Inversion of Coassembled Supramolecular Chirality through 2D-Sheet to Rolled-Up Tubular Structure. Journal of the American Chemical Society, 2017, 139, 17711-17714.	13.7	62
121	Reaction Mechanism of Area-Selective Atomic Layer Deposition for Al <sub>2</sub> O <sub>3</sub> Nanopatterns. ACS Applied Materials & Interfaces, 2017, 9, 41607-41617.	8.0	73
122	Highly Uniform Atomic Layer-Deposited MoS <sub>2</sub> @3D-Ni-Foam: A Novel Approach To Prepare an Electrode for Supercapacitors. ACS Applied Materials & Interfaces, 2017, 9, 40252-40264.	8.0	117
123	Zinc–Phosphorus Complex Working as an Atomic Valve for Colloidal Growth of Monodisperse Indium Phosphide Quantum Dots. Chemistry of Materials, 2017, 29, 6346-6355.	6.7	53
124	Uniform color coating of multilayered TiO2/Al2O3 films by atomic layer deposition. Journal of Coatings Technology Research, 2017, 14, 177-183.	2.5	4
125	Self-Limiting Layer Synthesis of Transition Metal Dichalcogenides. Scientific Reports, 2016, 6, 18754.	3.3	74
126	Comparison of hydrogen sulfide gas and sulfur powder for synthesis of molybdenum disulfide nanosheets. Current Applied Physics, 2016, 16, 691-695.	2.4	15

#	Article	IF	CITATIONS
127	High efficiency n-Si/p-Cu2O core-shell nanowires photodiode prepared by atomic layer deposition of Cu2O on well-ordered Si nanowires array. Electronic Materials Letters, 2016, 12, 404-410.	2.2	14
128	Effects of TaN Diffusion Barrier on Cu-Gate ZnO:N Thin-Film Transistors. IEEE Electron Device Letters, 2016, 37, 599-602.	3.9	4
129	Very high frequency plasma reactant for atomic layer deposition. Applied Surface Science, 2016, 387, 109-117.	6.1	13
130	Effect of Al <sub>2</sub> O <sub>3</sub> Deposition on Performance of Top-Gated Monolayer MoS <sub>2</sub> -Based Field Effect Transistor. ACS Applied Materials & Interfaces, 2016, 8, 28130-28135.	8.0	40
131	Improvement of Gas-Sensing Performance of Large-Area Tungsten Disulfide Nanosheets by Surface Functionalization. ACS Nano, 2016, 10, 9287-9296.	14.6	351
132	Highly conductive and flexible fiber for textile electronics obtained by extremely low-temperature atomic layer deposition of Pt. NPG Asia Materials, 2016, 8, e331-e331.	7.9	51
133	Highly Flexible Hybrid CMOS Inverter Based on Si Nanomembrane and Molybdenum Disulfide. Small, 2016, 12, 5720-5727.	10.0	46
134	Flexible Electronics: Highly Flexible Hybrid CMOS Inverter Based on Si Nanomembrane and Molybdenum Disulfide (Small 41/2016). Small, 2016, 12, 5650-5650.	10.0	0
135	High-Throughput Screening to Investigate the Relationship between the Selectivity and Working Capacity of Porous Materials for Propylene/Propane Adsorptive Separation. Journal of Physical Chemistry C, 2016, 120, 24224-24230.	3.1	37
136	Formation of Ni silicide from atomic layer deposited Ni. Current Applied Physics, 2016, 16, 720-725.	2.4	4
137	Uniform, large-area self-limiting layer synthesis of tungsten diselenide. 2D Materials, 2016, 3, 014004.	4.4	40
138	Static and Dynamic Performance of Complementary Inverters Based on Nanosheet α-MoTe <sub>2</sub> <i>p</i> -Channel and MoS <sub>2</sub> <i>n</i> -Channel Transistors. ACS Nano, 2016, 10, 1118-1125.	14.6	98
139	Growth characteristics and electrical properties of SiO2 thin films prepared using plasma-enhanced atomic layer deposition and chemical vapor deposition with an aminosilane precursor. Journal of Materials Science, 2016, 51, 5082-5091.	3.7	31
140	A Separate Extraction Method for Asymmetric Source and Drain Resistances Using Frequency-Dispersive C-V Characteristics in Exfoliated MoS <sub>2</sub> FET. IEEE Electron Device Letters, 2016, 37, 231-233.	3.9	7
141	Effects of Cl-Based Ligand Structures on Atomic Layer Deposited HfO <sub>2</sub> . Journal of Physical Chemistry C, 2016, 120, 5958-5967.	3.1	18
142	Wafer-scale, conformal and direct growth of MoS2 thin films by atomic layer deposition. Applied Surface Science, 2016, 365, 160-165.	6.1	119
143	Highâ€performance alternating current electroluminescent layers solution blended with mechanically and electrically robust nonradiating polymers. Journal of Polymer Science, Part B: Polymer Physics, 2015, 53, 1629-1640.	2.1	4
144	Fabrication and Experimental Analysis of 6.6 kV/100 A Class Single-Phase Superconducting Fault Current Controller With Superconducting DC Reactor Coil. IEEE Transactions on Applied Superconductivity, 2015, 25, 1-5.	1.7	1

Нуимсјим Кім

#	Article	IF	CITATIONS
145	Highly-conformal p-type copper(I) oxide (Cu2O) thin films by atomic layer deposition using a fluorine-free amino-alkoxide precursor. Applied Surface Science, 2015, 349, 673-682.	6.1	35
146	In situ surface cleaning on a Ge substrate using TMA and MgCp <sub>2</sub> for HfO <sub>2</sub> -based gate oxides. Journal of Materials Chemistry C, 2015, 3, 4852-4858.	5.5	20
147	Optimization and device application potential of oxide–metal–oxide transparent electrode structure. RSC Advances, 2015, 5, 65094-65099.	3.6	17
148	Lowering contact resistance by SWCNT–Al bilayer electrodes in solution processable metal-oxide thin film transistor. Journal of Materials Chemistry C, 2015, 3, 1403-1407.	5.5	3
149	Growth characteristics and properties of indium oxide and indium-doped zinc oxide by atomic layer deposition. Thin Solid Films, 2015, 587, 83-87.	1.8	19
150	Plasma-enhanced atomic layer deposition of Co on metal surfaces. Surface and Coatings Technology, 2015, 264, 60-65.	4.8	8
151	Real-time detection of chlorine gas using Ni/Si shell/core nanowires. Nanoscale Research Letters, 2015, 10, 18.	5.7	9
152	Controllable synthesis of molybdenum tungsten disulfide alloy for vertically composition-controlled multilayer. Nature Communications, 2015, 6, 7817.	12.8	188
153	Characterization of HfO N thin film formation by in-situ plasma enhanced atomic layer deposition using NH3 and N2 plasmas. Applied Surface Science, 2015, 349, 757-762.	6.1	14
154	Growth characteristics of graphene synthesized via chemical vapor deposition using carbon tetrabromide precursor. Applied Surface Science, 2015, 343, 128-132.	6.1	8
155	Nitrogen-doped ZnO/n-Si core–shell nanowire photodiode prepared by atomic layer deposition. Materials Science in Semiconductor Processing, 2015, 33, 154-160.	4.0	19
156	The impact of atomic layer deposited SiO <sub>2</sub> passivation for high-k Ta <sub>1â^'x</sub> Zr <sub>x</sub> O on the InP substrate. Journal of Materials Chemistry C, 2015, 3, 10293-10301.	5.5	13
157	Nucleation and Growth of the HfO <sub>2</sub> Dielectric Layer for Graphene-Based Devices. Chemistry of Materials, 2015, 27, 5868-5877.	6.7	43
158	Hydrophobicity of Rare Earth Oxides Grown by Atomic Layer Deposition. Chemistry of Materials, 2015, 27, 148-156.	6.7	106
159	Layer-modulated synthesis of uniform tungsten disulfide nanosheet using gas-phase precursors. Nanoscale, 2015, 7, 1308-1313.	5.6	86
160	Synthesis of carbon nanotube–nickel nanocomposites using atomic layer deposition for high-performance non-enzymatic glucose sensing. Biosensors and Bioelectronics, 2015, 63, 325-330.	10.1	150
161	Vapor Deposition Techniques for Synthesis of Two-Dimensional Transition Metal Dichalcogenides. Applied Microscopy, 2015, 45, 119-125.	1.4	7
162	Coupled self-assembled monolayer for enhancement of Cu diffusion barrier and adhesion properties. RSC Advances, 2014, 4, 60123-60130.	3.6	22

#	Article	IF	CITATIONS
163	Review of plasma-enhanced atomic layer deposition: Technical enabler of nanoscale device fabrication. Japanese Journal of Applied Physics, 2014, 53, 03DA01.	1.5	79
164	Atomic layer deposition of Y2O3 and yttrium-doped HfO2 using a newly synthesized Y(iPrCp)2(N-iPr-amd) precursor for a high permittivity gate dielectric. Applied Surface Science, 2014, 297, 16-21.	6.1	54
165	Growth characteristics and properties of Ga-doped ZnO (GZO) thin films grown by thermal and plasma-enhanced atomic layer deposition. Applied Surface Science, 2014, 295, 260-265.	6.1	44
166	Investigation of atomic layer deposition of magnesium oxide on a CoFeB layer for three-dimensional magnetic tunneling junctions. Journal of Alloys and Compounds, 2014, 588, 716-719.	5.5	11
167	Atomic layer deposition of CeO2/HfO2 gate dielectrics on Ge substrate. Applied Surface Science, 2014, 321, 214-218.	6.1	12
168	Atomic layer deposition of B2O3/SiO2 thin films and their application in an efficient diffusion doping process. Journal of Materials Chemistry C, 2014, 2, 5805.	5.5	26
169	Graphene as an atomically thin barrier to Cu diffusion into Si. Nanoscale, 2014, 6, 7503-7511.	5.6	89
170	Synthesis of wafer-scale uniform molybdenum disulfide films with control over the layer number using a gas phase sulfur precursor. Nanoscale, 2014, 6, 2821.	5.6	166
171	Fabrication of Transferable Al <sub>2</sub> O <sub>3</sub> Nanosheet by Atomic Layer Deposition for Graphene FET. ACS Applied Materials & Interfaces, 2014, 6, 2764-2769.	8.0	16
172	Dye-Sensitized MoS <sub>2</sub> Photodetector with Enhanced Spectral Photoresponse. ACS Nano, 2014, 8, 8285-8291.	14.6	268
173	High efficiency n-ZnO/p-Si core–shell nanowire photodiode based on well-ordered Si nanowire array with smooth surface. Materials Science in Semiconductor Processing, 2014, 27, 297-302.	4.0	17
174	Significant Enhancement of the Dielectric Constant through the Doping of <scp><scp>CeO</scp></scp> <sub>2</sub> into <scp><for>HfO</for></scp> <sub>2</sub> by Atomic Layer Deposition. Journal of the American Ceramic Society, 2014, 97, 1164-1169.	3.8	18
175	ZnO homojunction core–shell nanorods ultraviolet photo-detecting diodes prepared by atomic layer deposition. Sensors and Actuators A: Physical, 2014, 210, 197-204.	4.1	17
176	The electrical properties of low pressure chemical vapor deposition Ga doped ZnO thin films depending on chemical bonding configuration. Applied Surface Science, 2014, 297, 125-129.	6.1	34
177	Growth of highly conformal ruthenium-oxide thin films with enhanced nucleation by atomic layer deposition. Journal of Alloys and Compounds, 2014, 610, 529-539.	5.5	18
178	Plasma enhanced atomic layer deposition of magnesium oxide as a passivation layer for enhanced photoluminescence of ZnO nanowires. Journal of Luminescence, 2014, 145, 307-311.	3.1	14
179	Back End of the Line. , 2014, , 209-238.		1
180	Direct imprinting of MoS2 flakes on a patterned gate for nanosheet transistors. Journal of Materials Chemistry C, 2013, 1, 7803.	5.5	50

Нуимсјим Кім

#	Article	IF	CITATIONS
181	Layer-Controlled, Wafer-Scale, and Conformal Synthesis of Tungsten Disulfide Nanosheets Using Atomic Layer Deposition. ACS Nano, 2013, 7, 11333-11340.	14.6	324
182	Alkali earth metal dopants for high performance and aqueous-derived ZnO TFT. RSC Advances, 2013, 3, 21339.	3.6	3
183	Nanosheet thickness-modulated MoS <sub>2</sub> dielectric property evidenced by field-effect transistor performance. Nanoscale, 2013, 5, 548-551.	5.6	83
184	Growth characteristics and electrical properties of Ta2O5 grown by thermal and O3-based atomic layer deposition on TiN substrates for metal–insulator–metal capacitor applications. Thin Solid Films, 2013, 542, 71-75.	1.8	22
185	The effect of La2O3-incorporation in HfO2 dielectrics on Ge substrate by atomic layer deposition. Applied Surface Science, 2013, 287, 349-354.	6.1	34
186	Atomic layer deposition of transition metals for silicide contact formation: Growth characteristics and silicidation. Microelectronic Engineering, 2013, 106, 69-75.	2.4	18
187	Plasma-enhanced atomic layer deposition of Co using Co(MeCp)2 precursor. Journal of Energy Chemistry, 2013, 22, 403-407.	12.9	23
188	Synthesis of Few-Layered Graphene Nanoballs with Copper Cores Using Solid Carbon Source. ACS Applied Materials & Interfaces, 2013, 5, 2432-2437.	8.0	62
189	Cu-Al alloy formation by thermal annealing of Cu/Al multilayer films deposited by cyclic metal organic chemical vapor deposition. Metals and Materials International, 2013, 19, 611-616.	3.4	6
190	UV–Visible Spectroscopic Analysis of Electrical Properties in Alkali Metalâ€Đoped Amorphous Zinc Tin Oxide Thinâ€Film Transistors. Advanced Materials, 2013, 25, 2994-3000.	21.0	93
191	Atomic Layer Deposition of Ru Thin Films Using a Ru(0) Metallorganic Precursor and O <sub>2</sub> . ECS Journal of Solid State Science and Technology, 2013, 2, P47-P53.	1.8	35
192	Exciton dynamics in atomically thin MoS <mml:math xmlns:mml="http://www.w3.org/1998/Math/MathML" display="inline"&gt;<mml:msub><mml:mrow /&gt;<mml:mn>2</mml:mn></mml:mrow </mml:msub>: Interexcitonic interaction and broadening kinetics. Physical Review B, 2013, 88, .</mml:math 	3.2	173
193	Ru nanodot synthesis using CO2 supercritical fluid deposition. Journal of Physics and Chemistry of Solids, 2013, 74, 664-667.	4.0	5
194	Formation of Vertically Aligned Cobalt Silicide Nanowire Arrays Through a Solid-State Reaction. IEEE Nanotechnology Magazine, 2013, 12, 704-711.	2.0	5
195	n-ZnO:N/p-Si nanowire photodiode prepared by atomic layer deposition. Applied Physics Letters, 2012, 100, .	3.3	32
196	Low temperature atomic layer deposited Al-doped ZnO thin films and associated semiconducting properties. Journal of Vacuum Science and Technology B:Nanotechnology and Microelectronics, 2012, 30, 031210.	1.2	25
197	Silicidation of Co/Si Core Shell Nanowires. Journal of the Electrochemical Society, 2012, 159, K146-K151.	2.9	6
198	Selective epitaxial growth of Si1â^'xGex films via the alternating gas supply of Si2H6, GeH4, and Cl2: Effects of Cl2 exposure. Materials Letters, 2012, 88, 89-92.	2.6	0

#	Article	IF	CITATIONS
199	Facile fabrication of ordered Si1â^'xGex nanostructures via hybrid process of selective epitaxial growth (SEG) and self-assembled nanotemplates. Journal of Alloys and Compounds, 2012, 536, 166-172.	5.5	2
200	Gap-filling of Cu–Al alloy into nanotrenches by cyclic metalorganic chemical vapor deposition. Materials Research Bulletin, 2012, 47, 2961-2965.	5.2	2
201	Selective Area Atomic Layer Deposited ZnO Nanodot on Self-Assembled Monolayer Pattern Using a Diblock Copolymer Nano-Template. Journal of Nanoscience and Nanotechnology, 2012, 12, 1483-1486.	0.9	2
202	MoS <sub>2</sub> Nanosheet Phototransistors with Thickness-Modulated Optical Energy Gap. Nano Letters, 2012, 12, 3695-3700.	9.1	1,221
203	Initial Stage Growth during Plasmaâ€Enhanced Atomic Layer Deposition of Cobalt. Chemical Vapor Deposition, 2012, 18, 41-45.	1.3	19
204	Atomic Layer Deposition of Ni Thin Films and Application to Area-Selective Deposition. Journal of the Electrochemical Society, 2011, 158, D1.	2.9	79
205	Atomic layer deposition for nanoscale contact applications. , 2011, , .		1
206	Transparent conductive oxide film formed with a self textured surface for solar cell application. AIP Conference Proceedings, 2011, , .	0.4	0
207	Photocatalytic effect of thermal atomic layer deposition of TiO2 on stainless steel. Applied Catalysis B: Environmental, 2011, 104, 6-11.	20.2	32
208	The properties of plasma-enhanced atomic layer deposition (ALD) ZnO thin films and comparison with thermal ALD. Applied Surface Science, 2011, 257, 3776-3779.	6.1	108
209	Characteristics and applications of plasma enhanced-atomic layer deposition. Thin Solid Films, 2011, 519, 6639-6644.	1.8	83
210	Electrical and Optical Properties of Low Pressure Chemical Vapor Deposited Al-Doped ZnO Transparent Conductive Oxide for Thin Film Solar Cell. Journal of the Electrochemical Society, 2011, 158, D191.	2.9	8
211	Low Pressure Chemical Vapor Deposition of Aluminum-Doped Zinc Oxide for Transparent Conducting Electrodes. Journal of the Electrochemical Society, 2011, 158, D495.	2.9	45
212	Atomic layer deposition ZnO:N flexible thin film transistors and the effects of bending on device properties. Applied Physics Letters, 2011, 98, .	3.3	44
213	Growth Characteristics and Film Properties of Cerium Dioxide Prepared by Plasma-Enhanced Atomic Layer Deposition. Journal of the Electrochemical Society, 2011, 158, G169.	2.9	30
214	Atomic Layer Deposition of Co Using N2â^•H2 Plasma as a Reactant. Journal of the Electrochemical Society, 2011, 158, H1179.	2.9	33
215	Supercritical Fluid Deposition of SiO2Thin Films: Growth Characteristics and Film Properties. Journal of the Electrochemical Society, 2011, 159, D46-D49.	2.9	5
216	Programming and Erasing Operations of Nitride-Nitride-Oxynitride Stacked Thin Film Transistor Device. Journal of the Electrochemical Society, 2011, 158, H166.	2.9	0

#	Article	IF	CITATIONS
217	<i>In-Situ</i> Synchrotron X-Ray Scattering Study of Thin Film Growth by Atomic Layer Deposition. Journal of Nanoscience and Nanotechnology, 2011, 11, 1577-1580.	0.9	5
218	Electronic Structure of Cerium Oxide Gate Dielectric Grown by Plasma-Enhanced Atomic Layer Deposition. Journal of the Electrochemical Society, 2011, 158, G217.	2.9	41
219	A HfO2 Thin Film Resistive Switch Based on Conducting Atomic Force Microscopy. Electrochemical and Solid-State Letters, 2011, 14, H311.	2.2	15
220	The Effects of Ultraviolet Exposure on the Device Characteristics of Atomic Layer Deposited-ZnO:N Thin Film Transistors. Journal of the Electrochemical Society, 2011, 158, J150-J154.	2.9	25
221	Inductively Coupled-plasma Dry Etching of a ZnO Thin Film by Ar-diluted CF4 Gas. Journal of the Korean Physical Society, 2011, 58, 1536-1540.	0.7	12
222	Low-temperature Atomic Layer Deposition of TiO2, Al2O3, and ZnO Thin Films. Journal of the Korean Physical Society, 2011, 59, 452-457.	0.7	54
223	Synthesis of Si Nanowires by Using Atmospheric Pressure Chemical Vapor Deposition with SiCl4. Journal of the Korean Physical Society, 2011, 59, 485-488.	0.7	5
224	Room temperature ferroelectric property of BiMnO3 thin film with double SrTiO3 buffer layers on Pt/Ti/SiO2/Si substrate. Metals and Materials International, 2010, 16, 289-292.	3.4	13
225	Self-formation of dielectric layer containing CoSi2 nanocrystals by plasma-enhanced atomic layer deposition. Journal of Crystal Growth, 2010, 312, 2215-2219.	1.5	16
226	Electrical transport properties in electroless-etched Si nanowire field-effect transistors. Microelectronic Engineering, 2010, 87, 2407-2410.	2.4	16
227	Fabrication of rough Al doped ZnO films deposited by low pressure chemical vapor deposition for high efficiency thin film solar cells. Current Applied Physics, 2010, 10, S459-S462.	2.4	110
228	Optical and electrical properties of 2wt.% Al2O3-doped ZnO films and characteristics of Al-doped ZnO thin-film transistors with ultra-thin gate insulators. Thin Solid Films, 2010, 518, 2808-2811.	1.8	43
229	Photocatalytic activities of TiO2 thin films prepared on Galvanized Iron substrate by plasma-enhanced atomic layer deposition. Thin Solid Films, 2010, 518, 4757-4761.	1.8	20
230	Growth characteristics and electrical properties of La2O3 gate oxides grown by thermal and plasma-enhanced atomic layer deposition. Thin Solid Films, 2010, 519, 362-366.	1.8	57
231	The formation of sub-10nm nanohole array on block copolymer thin films on gold surface using surface neutralization based on O2 plasma treatment and self-assembled monolayer. Surface Science, 2010, 604, 1034-1039.	1.9	2
232	Plasma-Enhanced Atomic Layer Deposition of Ni. Japanese Journal of Applied Physics, 2010, 49, 05FA11.	1.5	38
233	Atomic Layer Deposition ZnO:N Thin Film Transistor: The Effects of N Concentration on the Device Properties. Journal of the Electrochemical Society, 2010, 157, H214.	2.9	52
234	High Quality Area-Selective Atomic Layer Deposition Co Using Ammonia Gas as a Reactant. Journal of the Electrochemical Society, 2010, 157, D10.	2.9	65

#	Article	IF	CITATIONS
235	The Effects of UV Exposure on Plasma-Enhanced Atomic Layer Deposition ZnO Thin Film Transistor. Electrochemical and Solid-State Letters, 2010, 13, H151.	2.2	14
236	Plasma-Enhanced Atomic Layer Deposition of Cobalt Using Cyclopentadienyl Isopropyl Acetamidinato-Cobalt as a Precursor. Japanese Journal of Applied Physics, 2010, 49, 05FA10.	1.5	42
237	Kelvin probe force microscopy for conducting nanobits of NiO thin films. Nanotechnology, 2010, 21, 215704.	2.6	10
238	Flatband voltage control in p-metal gate metal-oxide-semiconductor field effect transistor by insertion of TiO2 layer. Applied Physics Letters, 2010, 96, .	3.3	14
239	NiO Resistive Random Access Memory Nanocapacitor Array on Graphene. ACS Nano, 2010, 4, 2655-2658.	14.6	171
240	Multiferroic Properties of Highly c-Oriented BiFeO[sub 3] Thin Films on Glass Substrates. Electrochemical and Solid-State Letters, 2010, 13, G5.	2.2	9
241	Reduction of Electrical Hysteresis in Cyclically Bent Organic Field Effect Transistors by Incorporating Multistack Hybrid Gate Dielectrics. Journal of the Electrochemical Society, 2010, 157, H1046.	2.9	13
242	Flat band voltage (VFB) modulation by controlling compositional depth profile in La2O3/HfO2 nanolaminate gate oxide. Journal of Applied Physics, 2010, 107, 074109.	2.5	27
243	?The Degradation of Deposition Blocking Layer during Area Selective Plasma Enhanced Atomic Layer Deposition of Cobalt. Journal of the Korean Physical Society, 2010, 56, 104-107.	0.7	26
244	The Surface Morphology of ZnO Grown by Metal Organic Chemical Vapor Deposition for an Application of Solar Cell. Applied Science and Convergence Technology, 2010, 19, 177-183.	0.9	2
245	SiGe nanostructure fabrication through selective epitaxial growth using self-assembled nanotemplates. IOP Conference Series: Materials Science and Engineering, 2009, 6, 012019.	0.6	0
246	Effects of Fluorine Plasma Treatment on the Electronic Structure of Plasma-Enhanced Atomic Layer Deposition HfO[sub 2]. Journal of the Electrochemical Society, 2009, 156, G33.	2.9	9
247	HfO[sub 2]/HfO[sub x]N[sub y]/HfO[sub 2] Gate Dielectric Fabricated by In Situ Oxidation of Plasma-Enhanced Atomic Layer Deposition HfN Middle Layer. Journal of the Electrochemical Society, 2009, 156, G109.	2.9	16
248	Supercritical Fluid Deposition of Conformal SrTiO[sub 3] Films with Composition Uniformity in Nanocontact Holes. Electrochemical and Solid-State Letters, 2009, 12, D45.	2.2	12
249	Plasma-Enhanced ALD of TiO[sub 2] Thin Films on SUS 304 Stainless Steel for Photocatalytic Application. Journal of the Electrochemical Society, 2009, 156, D188.	2.9	14
250	Interface roughness effect between gate oxide and metal gate on dielectric property. Thin Solid Films, 2009, 517, 3892-3895.	1.8	11
251	Applications of atomic layer deposition to nanofabrication and emerging nanodevices. Thin Solid Films, 2009, 517, 2563-2580.	1.8	533
252	Epitaxially strained Na0.7CoO2 thin films on SrTiO3 buffer layer. Journal of Crystal Growth, 2009, 311, 1021-1024.	1.5	1

#	Article	IF	CITATIONS
253	Photocatalytic functional coatings of TiO2 thin films on polymer substrate by plasma enhanced atomic layer deposition. Applied Catalysis B: Environmental, 2009, 91, 628-633.	20.2	70
254	Heteroepitaxial Ferroelectric ZnSnO <sub>3</sub> Thin Film. Journal of the American Chemical Society, 2009, 131, 8386-8387.	13.7	93
255	Dip-Pen Lithography of Ferroelectric PbTiO <sub>3</sub> Nanodots. Journal of the American Chemical Society, 2009, 131, 14676-14678.	13.7	57
256	Cobalt and nickel atomic layer depositions for contact applications. , 2009, , .		2
257	Atomic Layer Deposition of Ruthenium and Ruthenium-oxide ThinFilms by Using a Ru(EtCp)\$_{2}\$ Precursor and Oxygen Gas. Journal of the Korean Physical Society, 2009, 55, 32-37.	0.7	41
258	ZnO thin films prepared by atomic layer deposition and rf sputtering as an active layer for thin film transistor. Thin Solid Films, 2008, 516, 1523-1528.	1.8	132
259	Effect oxygen exposure on the quality of atomic layer deposition of ruthenium from bis(cyclopentadienyl)ruthenium and oxygen. Thin Solid Films, 2008, 516, 7345-7349.	1.8	45
260	Spontaneous Formation of Vertical Magneticâ€Metalâ€Nanorod Arrays During Plasmaâ€Enhanced Atomic Layer Deposition. Small, 2008, 4, 2247-2254.	10.0	32
261	Evaluation of bone healing with eggshellâ€derived bone graft substitutes in rat calvaria: A pilot study. Journal of Biomedical Materials Research - Part A, 2008, 87A, 203-214.	4.0	63
262	Thin film growth and magnetic anisotropy of epitaxial Sr0.775Y0.225CoO3â^î. Journal of Crystal Growth, 2008, 310, 3649-3652.	1.5	8
263	Improvement of the contact resistance between ITO and pentacene using various metal-oxide interlayers. Organic Electronics, 2008, 9, 1140-1145.	2.6	14
264	Thermal and plasma enhanced atomic layer deposition ruthenium and electrical characterization as a metal electrode. Microelectronic Engineering, 2008, 85, 39-44.	2.4	89
265	Synthesis of horizontally aligned ZnO nanowires localized at terrace edges and application for high sensitivity gas sensor. Applied Physics Letters, 2008, 93, .	3.3	67
266	Dendron-Modified Polystyrene Microtiter Plate: Surface Characterization with Picoforce AFM and Influence of Spacing between Immobilized Amyloid Beta Proteins. Langmuir, 2008, 24, 14296-14305.	3.5	15
267	Ru nanostructure fabrication using an anodic aluminum oxide nanotemplate and highly conformal Ru atomic layer deposition. Nanotechnology, 2008, 19, 045302.	2.6	79
268	Electrical Properties of Atomic Layer Deposition HfO[sub 2] and HfO[sub x]N[sub y] on Si Substrates with Various Crystal Orientations. Journal of the Electrochemical Society, 2008, 155, H267.	2.9	17
269	Hybrid nanofabrication processes utilizing diblock copolymer nanotemplate prepared by self-assembled monolayer based surface neutralization. Journal of Vacuum Science & Technology B, 2008, 26, 189.	1.3	20
270	The effects of nitrogen profile and concentration on negative bias temperature instability of plasma enhanced atomic layer deposition HfOxNy prepared by in situ nitridation. Journal of Applied Physics, 2008, 104, 064111.	2.5	12

#	Article	IF	CITATIONS
271	In-Situ Doping during ZnO Atomic Layer Deposition. Journal of the Korean Physical Society, 2008, 53, 253-257.	0.7	9
272	Comparative Studies of Atomic Layer Deposition and Plasma-Enhanced Atomic Layer Deposition Ta2O5and the Effects on Electrical Properties ofIn situNitridation. Japanese Journal of Applied Physics, 2007, 46, 3224-3228.	1.5	13
273	High quality epitaxial CoSi2 using plasma nitridation-mediated epitaxy: The effects of the capping layer. Journal of Applied Physics, 2007, 102, 094509.	2.5	3
274	High performance thin film transistor with low temperature atomic layer deposition nitrogen-doped ZnO. Applied Physics Letters, 2007, 91, .	3.3	166
275	Nitride mediated epitaxy of CoSi2 through self-interlayer-formation of plasma-enhanced atomic layer deposition Co. Applied Physics Letters, 2007, 90, 213509.	3.3	25
276	Dependence of electrical properties on interfacial layer of Ta2O5 films. Microelectronic Engineering, 2007, 84, 2865-2868.	2.4	7
277	Thermal and Plasma-Enhanced ALD of Ta and Ti Oxide Thin Films from Alkylamide Precursors. Electrochemical and Solid-State Letters, 2006, 9, G191.	2.2	83
278	The application of atomic layer deposition for metallization of 65 nm and beyond. Surface and Coatings Technology, 2006, 200, 3104-3111.	4.8	69
279	High-Quality Cobalt Thin Films by Plasma-Enhanced Atomic Layer Deposition. Electrochemical and Solid-State Letters, 2006, 9, G323.	2.2	90
280	High-Capacity, Self-Assembled Metal–Oxide–Semiconductor Decoupling Capacitors. IEEE Electron Device Letters, 2004, 25, 622-624.	3.9	89